Macromolecular Research
https://doi.org/10.1007/s13233-024-00344-9

Online ISSN 2092-7673
Print ISSN 1598-5032

COMMUNICATION

Polyacrylamide-based nanocomposite hydrogel prepared by synergistic solar light-induced polymerization

Nery M. Aguilar[1] · Brenda L. Sanchez-Gaytan[1] · Guillermo Soriano-Moro[1]

Received: 26 February 2024 / Revised: 30 October 2024 / Accepted: 11 November 2024

Abstract

A straightforward approach to prepare a nanocomposite hybrid hydrogel through simultaneous processes of nanoparticle formation, polymerization and crosslinking processes induced by sunlight is reported. This method requires just the gold precursor and acrylamide monomers to form a hydrogel network without the need of any initiator or crosslinking agent. The synthesis is based on a synergistic approach where the acrylamide monomer (AM) acts as a reducing agent and capping ligand to obtain gold nanoparticles (AuNPs), while the presence of these nanostructures induce both the polymerization and the crosslinking process.

Graphical abstract

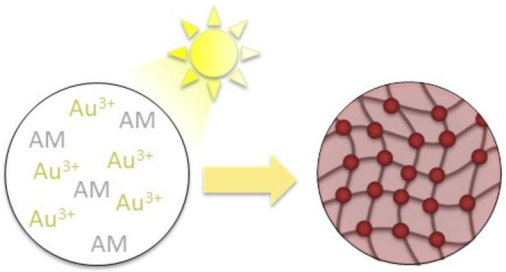

Easy formation of Au nanoparticles and hydrogel by solar light

Keywords Polyacrylamide hydrogel · Nanocomposites · Gold nanoparticles

1 Introduction

New technologies demand not only new materials with a variety of different features and characteristics but also novel ways to modulate such desired physicochemical properties. Achieving such tailored materials requires the incorporation of new components during the process of synthesis. Particularly, in the generation of polymer-based materials, the integration of inorganic nanostructures within a polymeric matrix to create nanocomposites, has proven to be an effective way of including and tuning new material properties. An attractive element during the generation of new materials is the harness of solar radiation to carry out different types of processes due to its plentiful availability and reduced environmental impact [1, 2]. Hydrogels, polymeric macromolecular networks capable to contain large amounts of water within the interstitial spaces of its array, represent one of the most adaptable and attractive materials with innovative applications in many different fields [3]. Their remarkable features, including biocompatibility, permeable-soft structure, and good mechanical behavior, make them

✉ Brenda L. Sanchez-Gaytan
brendale.sanchez@correo.buap.mx

✉ Guillermo Soriano-Moro
jesus.soriano@correo.buap.mx

[1] Centro de Química, Instituto de Ciencias, Benemérita Universidad Autónoma de Puebla (BUAP), 72570 Puebla, México

Published online: 08 January 2025

versatile materials for biomedical and environmental applications. These properties are strongly related with the chemical nature of the polymer and the crosslinker, which are responsible for the macromolecular arrangement [4–6] and, in the case of nanocomposite hydrogels, the nanostructure also imprints additional and relevant features [7, 8]. Among the many advantageous properties of this type of composite materials, mechanical reinforcement, biofunctionality and susceptibility to electromagnetic fields are some of the most sought after [9–11]. In addition, like in any composite material, a homogeneous distribution and a strong interaction between both components, hydrogel and nanostructures, should be assured [12–14]. Homogeneity within the structure can be achieved if the nanoparticles are involved during the hydrogel formation process.

One straightforward and novel approach to carry out this goal is the photopolymerization promoted by nanostructures [15]. In this process, as its name implies, photoresponsive nanoparticles interact with electromagnetic radiation to initiate the polymerization [16]. In certain cases, these nanoparticles can also act as crosslinking entities for the growing polymeric chains, generating a polymer network which gives rise to the formation of a hydrogel [17]. However, to the best of our knowledge, only semiconductor nanomaterials have been used for this purpose and there is still a lack of information on how the network formation occurs [15–17]. In this work, we used gold nanoparticles (AuNPs) as photoinitiator to yield polyacrylamide hybrid nanocomposite hydrogels through sunlight radiation. Here, like the initiation mechanism of semiconductor species, plasmonic nanoparticles such as AuNPs are able to promote the initiation of the polymerization due to their localized surface plasmon resonance (LSPR) [18]. This process is known as plasmon-induced polymerization and to date, it has not been used to prepare hydrogels [19, 20]. Importantly, in contrast with common strategies where premade nanoparticles are used, in this synergistic approach, an aqueous solution of the monomer and the metal precursor were used. Thus, the monomer acts as a reducing and capping agent to form the nanoparticles and these nanostructures induce the monomer polymerization and crosslinking processes. Therefore, this is the first report where a synergist plasmon-induced polymerization-crosslinking process is used to obtain hybrid hydrogels.

2 Experimental

2.1 Materials

Acrylamide monomer (AM; ≥ 99%), and Gold (III) chloride solution ($HAuCl_4$; ≥ 99.9%) were acquired from Sigma-Aldrich. Chloroform used for the acrylamide recrystallization was purchased from Fermont (Monterrey, Mexico).

2.2 Synthesis procedures

2.2.1 Hydrogel synthesis varying AM concentration

Acrylamide, previously recrystallized in chloroform, was solubilized in the metal precursor solution (8 mL; 0.5 mM) within a conical plastic tube and placed under midday sunlight during one hour. The average solar radiation was 600–900 W/m^2 (19°02′N 98°11′N). The products obtained were extracted from the tube, washed with methanol and dried at room temperature; the reaction conditions are summarized in Table 1.

2.2.2 Hydrogel synthesis varying gold precursor concentration

Acrylamide monomer, 28 mmol, previously recrystallized in chloroform was used (Table 2). The monomer was solubilized in the metal precursor solution (8 mL; at different concentrations) within a conical plastic tube and placed under sunlight during 1 h. The products obtained were extracted from the tube, washed with methanol and dried at room temperature during 24 h.

2.3 Characterization

Attenuated Total Reflectance-Fourier Transform Infrared Spectroscopy (ATR–FTIR) measurements were performed in a Cary 630 spectrometer (Agilent Technologies) using a universal attenuated total reflectance (ATR) accessory. The hydrogels were analyzed completely dehydrated at 60 °C. UV–Vis spectroscopy measurements were carried out on a Varian Cary 50 spectrophotometer (Agilent Technologies) with a xenon lamp. In this analysis, a quartz cuvette was not

Table 1 Conditions used to produce the hydrogel varying the acrylamide concentration

Label	AM (M)	$HAuCl_4$ (mM)	Hydrogel formation	Reaction time (h)
HAM-Au-a	3.5	0.5	✓	1
HAM-Au-b	1.75		Partially	
HAM-Au-c*	0.87		×	
HAM-Au-d*	0.44		×	

*These conditions were tested by increasing the reaction time up to 2 h without success

Table 2 Conditions used to produce the hydrogel varying the gold precursor concentration

Label	AM (M)	$HAuCl_4$ (mM)	Hydrogel formation	Reaction time (h)
H1AM-Au	3.5	0.26	✓	1
H2AM-Au		0.13	✓	
H3AM-Au		0.065	✓	
H4AM-Au		0.032	Viscous solution	
H5AM-Au*		0.016	×	
H6AM-Au*		0.008	×	
H7AM-Au*		0.004	×	
H8AM-Au*		0.002	×	

*These conditions were tested also by increasing the reaction time up to 2 h without success

used since only the gel was introduced into the sample site. Scanning transmission electron microscopy (STEM) micrographs were acquired with 30 kV using a JSM-7800F scanning electron microscope (JEOL Ltd). The samples were cut transversely using cryogenics.

For SEM, a small amount of lyophilized sample was placed on conductive double-sided carbon tape (nisshimem) and then, was gold coated at 0.1 Torr and 5 s of plasma exposure using a SPI Module™ Sputter Coater. The samples were observed in a JEOL Field Emission Gun-Scanning Electron Microscope model JSM 7800 F at 1 kV of acceleration voltage and 6 mm working distance. An Everhart–Thornley detector mounted in the chamber was used for surface analysis. UV–Vis spectroscopy measurements were carried out on a Lambda 20 spectrophotometer (Perkin Elmer).

3 Results and discussion

Acrylamide monomers act as very effective reducing agents to produce gold nanoparticles [21], which is evidenced by the formation of intense coloration even at low monomer concentrations (Table 1). After the gold precursor reduction, the AuNPs start to nucleate and grow to form the nanostructure with a final size and morphology determined by the characteristics and concentration of the capping ligands, in this case AM monomers. Once formed, these nanostructures are able to couple with solar radiation to generate a localized coherent oscillation of surface electrons (LSPR) [22]. The light-excited surface electrons possess high energy that can be transferred to monomer molecules close to their surface [23, 24]. Therefore, the monomers attached to the nanoparticles surface can generate active species capable of initiating the growth of the polymer chains [25] (Scheme 1). Consequently, only monomers with available functional groups (i.e. low steric hindrance) and good affinity to the surface of the nanostructures are able to promote the polymerization reaction. Specifically, acrylamide monomer, used in this work, interacts favorably with the AuNPs since the primary amide, responsible for this interaction and also for the gold reduction, lacks bulky substituents that can affect its interaction with the AuNPs surface. Importantly, the nanoparticles surface can act as crosslinking sites for the subsequent hydrogel network development, which is formed even in the absence of a crosslinking external agent.

After the polymer growth is complete, the active species can be deactivated by combination. Thus, the polymer chains attached to AuNPs surface, can bind to each other effectively generating the pores of the nanocomposite hydrogel (Fig. 1A). As a result, the nanoparticles act as crosslinking points in this arrangement. STEM micrographs of a lateral

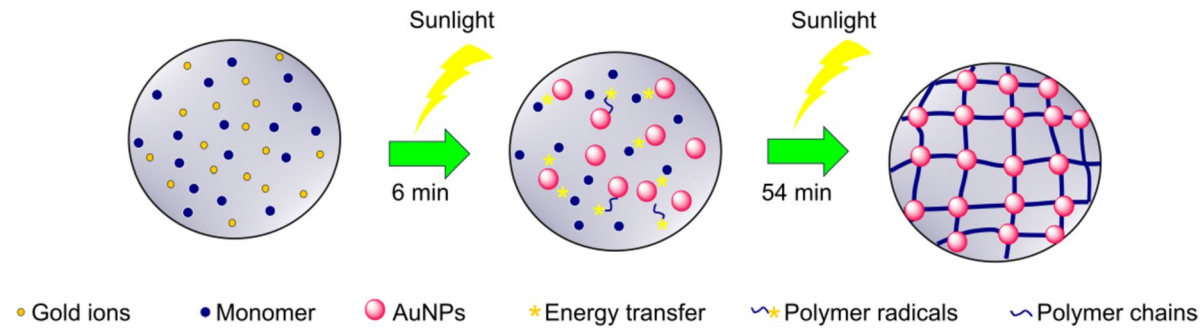

Scheme 1 Representation of the photopolymerization process induced by plasmonic nanoparticles

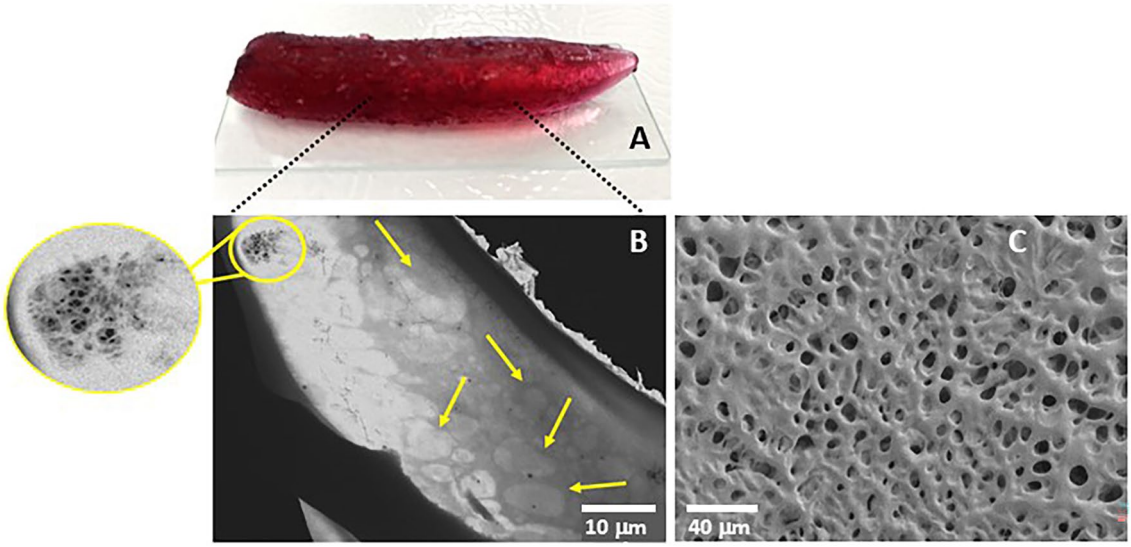

Fig. 1 Photograph of the polyacrylamide-gold nanoparticles hybrid hydrogel (**A**). STEM micrograph of a lateral section showing a close-up of gold nanoparticles and the pores (yellow arrows) (**B**). SEM micrograph of the lyophilized hydrogel showing the highly porous structure (**C**) (colour figure online)

cross section of the hydrogel (Fig. 1B) confirm the presence of gold nanoparticles of sizes between 5 and 25 nm, as well as the presence of micro-sized pores within the material (yellow arrows). SEM micrographs of a lyophilized hydrogel (Fig. 1C) show the highly structured porous nature of the material with an average pore size of 10 µm.

In this approach, an adequate distance between the nanostructures and the monomer must be ensured for the polymer-nanoparticle network to form. This can be achieved by modulating the concentrations of both the gold precursor and the acrylamide (Tables 1 and 2). It is important to mention that, since acrylamide also act as a reducing-capping agent, a decrease in the ratio capping-agent/gold-precursor causes changes in the size and morphologies of the nanostructures [26]. In addition, at low monomer concentration, while the nanoparticles are still formed, the monomer intermolecular distance is not adequate to form a network and the energy was not efficiently transferred from the surface of the nanoparticles to the acrylamide monomers, so the hydrogel is not obtained.

At this low-monomer concentration (< 0.9 mM), the deep purple color of the solution suggests the presence of larger non-spherical nanostructures or agglomerates. In contrast, at appropriate concentrations, the composite hydrogel displays a deep ruby red color, characteristic of the presence of spherical gold nanoparticles. UV–Vis spectroscopy shows that at higher than 1.75 mM monomer concentrations, sharp plasmon bands with a maximum of 530 nm, typical of 20 nm spherical nanoparticles, are observed (Fig. 2) [27]. Contrary to this, as monomer concentrations decrease, the plasmon bands widens and its maximum shifts to longer wavelenghts. At low monomer concentration (< 0.9 mM) the polymer is not formed, possibly because the energy necessary to promote the reaction, was not efficiently transferred from nanoparticles' LSPR to the acrylamide given their limited interaction. Under those conditions, a deep purple color solution, representative of heterogeneous and agglomerated nanoparticles, was observed. This result is consistent with having a good reducing agent but at those low polymer concentration there is not enough amount of polymer chains to effectively protect the newly formed nanoparticles.

On the other hand, the presence of gold nanostructures is indispensable to form the hydrogel. Thus, by decreasing the gold precursor concentration in the reaction, the color intensity of the solution also decreases, but a plasmon band at 530 nm can still be observed (Fig. 3). The absence of color in the solution indicates that the formation of the nanoparticles is no longer achieved. Therefore, neither nanostructures nor hydrogel were formed since the LSPR does not occur and the polymerization cannot be induced.

The structural analysis of the hydrogel by FT–IR (Fig. 4A), shows the vibrational bands related to the primary amine ($–NH_2$) at 3400 and 3200 cm^{-1}, the CH_2 of the polymer backbone at 2980 cm^{-1} and the C = O of the amide group at 1645 cm^{-1} and 1603 cm^{-1}. This confirms that the complete polymerization of acrylamide was achieved. Thermal degradation of this material was studied by TGA and DSC (Fig. 4B). The thermograms illustrate the complete dehydration of the hydrogel at 100 °C. Likewise, the transition close to 225 °C is likely due to the rupture of the surface interactions between the AuNPs crosslinkers and the polymer chains. This behavior is generated by the amide

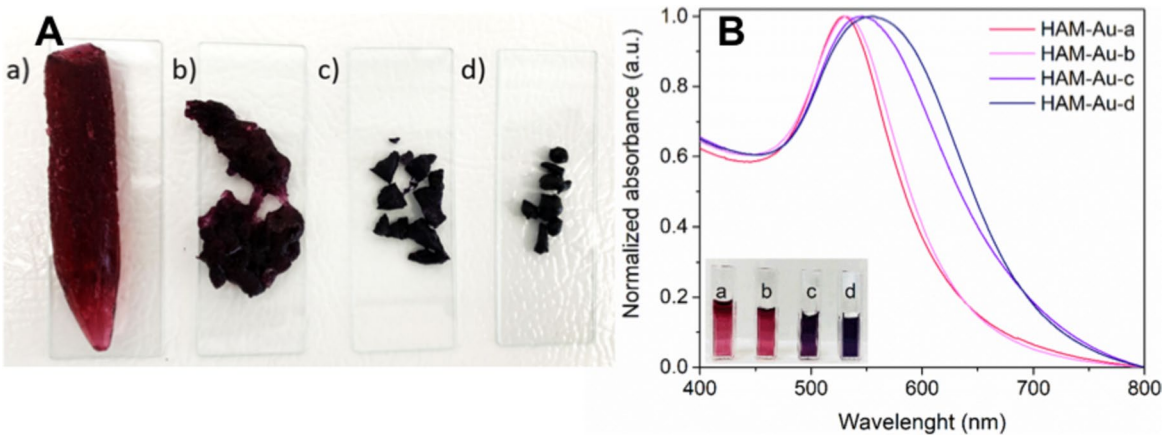

Fig. 2 **A** Images of the materials obtained at the following AM concentrations: **a** 3.5 mM, **b** 1.75 mM, **c** 0.87 mM and **d** 0.44 mM [from **a** hydrogel to **d** xerogel]. **B** UV–Vis spectra of hydrogels prepared at different monomer concentration. The labels correspond to the ones in Table 1

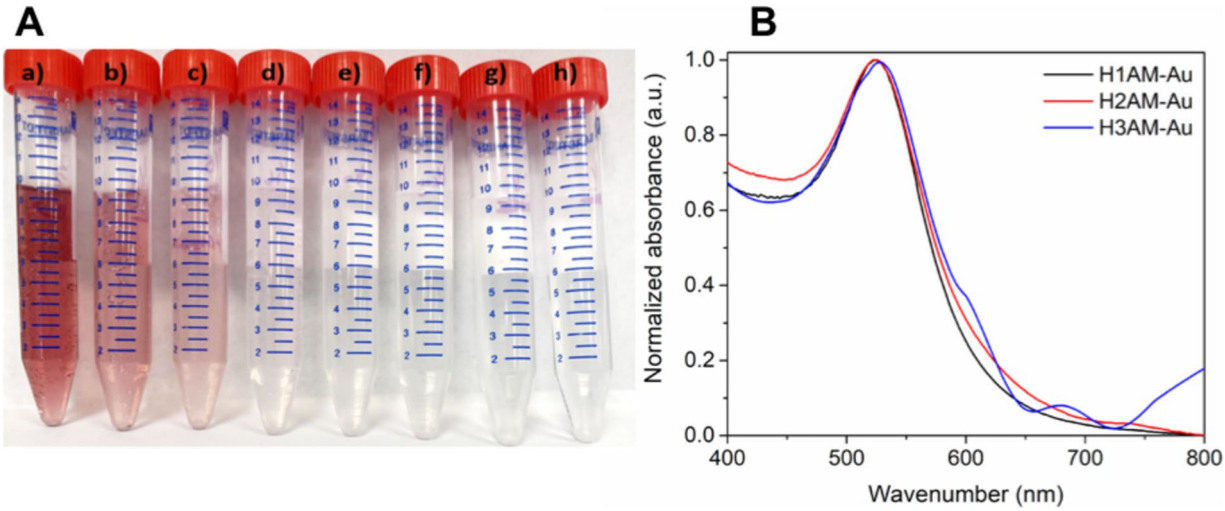

Fig. 3 **A** Materials obtained by varying the concentration of the gold precursor; **a** H1AM-Au, **b** H2AM-Au, **c** H3AM-Au, **d** H4AM-Au, **e** H5AM-Au, **f** H6AM-Au, **g** H7AM-Au, **h** H8AM-Au. **B** UV–Vis spectrum of the hydrogels obtained according to the conditions of Table 2, (a defined plasmon with a maximum at 530 nm is observed typically ≤ 20 nm of homogeneous spherical gold nanoparticles

decomposition into amines and imides as reported in the literature [28]. Imines have a large steric hindrance that blocks the interaction with the surface of the nanoparticles, so the crosslinking points are broken and the network collapses. So, from this temperature it is observed how the mass decreases until it reaches a minimum value.

4 Conclusions

A new approach to prepare a nanocomposite hydrogel based on gold precursor and acrylamide monomers is presented. The preparation of nanocomposite hydrogel was achieved using the physical phenomenon of localized surface plasmon resonance process (LSPR) exhibited by plasmonic nanoparticles. This novel approach takes advantage of the synergistic process of the formation of plasmonic nanoparticles, due to the reducing capacity of the acrylamide monomer, and the use of their localized surface plasmon resonance as a photoinitiator for the polymerization reaction and generation of a hydrogel. This method stands out for being simple and straightforward, for not using organic crosslinkers and instead employing the accessible and non-ending energy source that is sunlight.

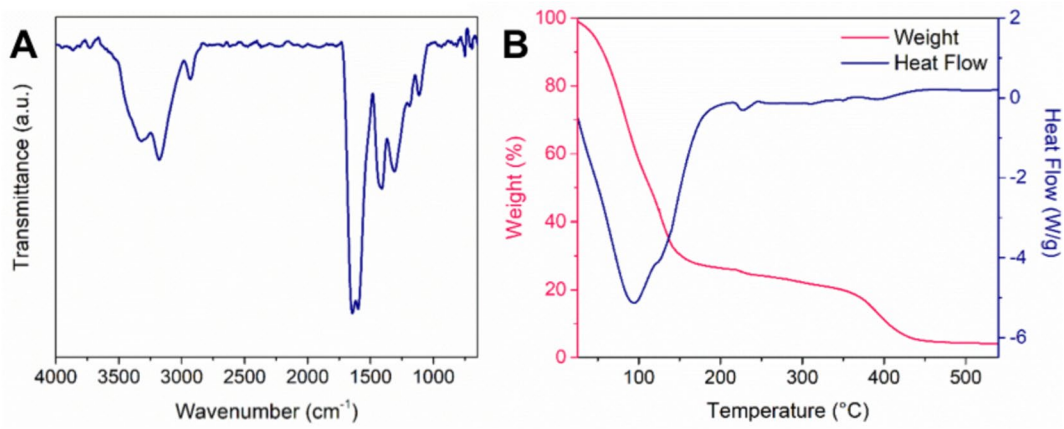

Fig. 4 **A** FT-IR spectrum of nanocomposite hydrogel. **B** Thermograms of TGA (red) and DSC (blue) obtained in the process of thermal degradation of the hydrogel (colour figure online)

Acknowledgements The authors thank to IFUAP and CNMN-IPN for their support in TGA-DSC, and STEM, respectively. Also, CONAHCyT-Mexico for financial support (N.M.A. Ph.D. fellowship No. 743248).

Funding This article is funded by VIEP-BUAP, projects 00364 and 00384.

Declarations

Conflict of interest The authors declare no conflicts of interest in this work.

References

1. A.H. Allah, H.A. Alshamsi, Facile green synthesis of ZnO/AC nanocomposites using Pontederia crassipes leaf extract and their photocatalytic properties based on visible light activation. J. Mater. Sci. Mater. Electron. (2023). https://doi.org/10.1007/s10854-023-10636-y
2. A. Al-nayili, H.A. Khayoon, H.A. Alshamsi, N.M. Cata Saady, A novel bimetallic (Au-Pd)-decorated reduced graphene oxide nanocomposite enhanced rhodamine B photocatalytic degradation under solar irradiation. Mater. Today Sustain. (2023). https://doi.org/10.1016/j.mtsust.2023.100512
3. S. Bashir, M. Hina, J. Iqbal, A.H. Rajpar, M.A. Mujtaba, N.A. Alghamdi, S. Wageh, K. Ramesh, S. Ramesh, Fundamental concepts of hydrogels: synthesis, properties, and their applications. Polymers (2020). https://doi.org/10.3390/polym12112702
4. W. Hu, Z. Wang, Y. Xiao, S. Zhang, J. Wang, Advances in crosslinking strategies of biomedical hydrogels. Biomater. Sci. (2019). https://doi.org/10.1039/C8BM01246F
5. X. Li, Q. Sun, Q. Li, N. Kawazoe, G. Chen, Functional hydrogels with tunable structures and properties for tissue engineering applications. Front. Chem. (2018). https://doi.org/10.3389/fchem.2018.00499
6. T. Kopač, A. Ručigaj, M. Krajnc, The mutual effect of the crosslinker and biopolymer concentration on the desired hydrogel properties. Int. J. Biol. Macromol. (2020). https://doi.org/10.1016/j.ijbiomac.2020.05.088
7. R. Esmaeely Neisiany, M.S. Enayati, P. Sajkiewicz, Z. Pahlevanneshan, S. Ramakrishna, Insight into the current directions in functionalized nanocomposite hydrogels. Front. Mater. (2020). https://doi.org/10.3389/fmats.2020.00025
8. Y. Jiang, N. Krishnan, J. Heo, R.H. Fang, L. Zhang, Nanoparticle-hydrogel superstructures for biomedical applications. J. Control. Release (2020). https://doi.org/10.1016/j.jconrel.2020.05.041
9. A. Chakraborty, A. Roy, S.P. Ravi, A. Paul, Exploiting the role of nanoparticles for use in hydrogel-based bioprinting applications: concept, design, and recent advances. Biomater. Sci. (2021). https://doi.org/10.1039/D1BM00605C
10. M.C. Arno, M. Inam, A.C. Weems, Z. Li, A.L.A. Binch, C.I. Platt, S.M. Richardson, J.A. Hoyland, A.P. Dove, R.K. O'Reilly, Exploiting the role of nanoparticle shape in enhancing hydrogel adhesive and mechanical properties. Nat. Commun. (2020). https://doi.org/10.1038/s41467-020-15206-y
11. C. Ferrag, S. Li, K. Jeon, N.M. Andoy, R.M.A. Sullan, S. Mikhaylichenko, K. Kerman, Polyacrylamide hydrogels doped with different shapes of silver nanoparticles: antibacterial and mechanical properties. Colloids Surfaces B Biointerfaces (2021). https://doi.org/10.1016/j.colsurfb.2020.111397
12. N.M. Aguilar, J.M. Perez-Aguilar, V.J. González-Coronel, J.G. Soriano-Moro, B.L. Sanchez-Gaytan, Polymers as versatile players in the stabilization, capping, and design of inorganic nanostructures. ACS Omega (2021). https://doi.org/10.1021/acsomega.1c05420
13. S. Merino, C. Martín, K. Kostarelos, M. Prato, E. Vázquez, Nanocomposite hydrogels: 3D polymer-nanoparticle synergies for on-demand drug delivery. ACS Nano (2015). https://doi.org/10.1021/acsnano.5b01433

14. U.S.K. Madduma-Bandarage, S.V. Madihally, Synthetic hydrogels: synthesis, novel trends, and applications. J. Appl. Polym. Sci. (2021). https://doi.org/10.1002/app.50376
15. S. Dadashi-Silab, A.M. Asiri, S.B. Khan, K.A. Alamry, Y. Yagci, Semiconductor nanoparticles for photoinitiation of free radical polymerization in aqueous and organic media. J. Polym. Sci. Part A Polym. Chem. (2014). https://doi.org/10.1002/pola.27145
16. Y. Zhu, E. Egap, Light-mediated polymerization induced by semiconducting nanomaterials: state-of-the-art and future perspectives. ACS Polym. Au (2021). https://doi.org/10.1021/acspolymersau.1c00014
17. D. Zhang, J. Yang, S. Bao, Q. Wu, Q. Wang, Semiconductor nanoparticle-based hydrogels prepared via self-initiated polymerization under sunlight. Even Visible Light. Sci. Rep. (2013). https://doi.org/10.1038/srep01399
18. Y. Wang, S. Wang, S. Zhang, O.A. Scherman, J.J. Baumberg, T. Ding, H. Xu, Plasmon-directed polymerization: regulating polymer growth with light. Nano Res. (2018). https://doi.org/10.1007/s12274-018-2163-0
19. K.C. Anyaogu, X. Cai, D.C. Neckers, Gold nanoparticle photopolymerization of acrylates. Macromolecules (2008). https://doi.org/10.1021/ma801391p
20. J. Zhang, M. Li, Y. He, X. Zhang, Z. Cui, P. Fu, M. Liu, X. Qiao, Q. Zhao, X. Pang, From 0-dimension to 1-dimensions: Au nanocrystals as versatile plasmonic photocatalyst for broadband light induced RAFT polymerization. Polym. Chem. (2021). https://doi.org/10.1039/D1PY00088H
21. M.N. Aguilar, J.M. Perez-Aguilar, V.J. González-Coronel, H. Martínez-Gutiérrez, T. Zayas Pérez, G. Soriano-Moro, B.L. Sanchez-Gaytan, Hydrolyzed polyacrylamide as an in situ assistant in the nucleation and growth of gold nanoparticles. Materials (2022). https://doi.org/10.3390/ma15238557
22. A. Furube, S. Hashimoto, Insight into plasmonic hot-electron transfer and plasmon molecular drive: new dimensions in energy conversion and nanofabrication. NPG Asia Mater. (2017). https://doi.org/10.1038/am.2017.191
23. C. Wang, D. Astruc, Nanogold plasmonic photocatalysis for organic synthesis and clean energy conversion. Chem. Soc. Rev. (2014). https://doi.org/10.1039/C4CS00145A
24. R.F. Ribeiro, L.A. Martínez-Martínez, M. Du, J. Campos-Gonzalez-Angulo, J. Yuen-Zhou, Polariton chemistry: controlling molecular dynamics with optical cavities. Chem. Sci. (2018). https://doi.org/10.1039/C8SC01043A
25. K.C. Anyaogu, X. Cai, D.C. Neckers, Gold nanoparticle photosensitized radical photopolymerization. Photochem. Photobiol. Sci. (2008). https://doi.org/10.1039/b812328d
26. J. Dong, P.L. Carpinone, G. Pyrgiotakis, P. Demokritou, B.M. Moudgil, Synthesis of precision gold nanoparticles using Turkevich method. KONA Powder Particle J. (2020). https://doi.org/10.14356/kona.2020011
27. X. Liu, M. Atwater, J. Wang, Q. Huo, Extinction coefficient of gold nanoparticles with different sizes and different capping ligands. Colloids Surfaces B Biointerfaces (2007). https://doi.org/10.1016/j.colsurfb.2006.08.005
28. H.D. Burrows, H.A. Ellis, S.I. Utah, Adsorbed metal ions as stabilizers for the thermal degradation of polyacrylamide. Polymer (1981). https://doi.org/10.1016/0032-3861(81)90397-9